ELSEVIER

Journal of Magnetism and Magnetic Materials 184 (1998) 41–48

journal of magnetism and magnetic materials

Preparation and magnetic properties of the CoO/Co bilayer

B. Raquet[a], R. Mamy[a,*], J.C. Ousset[a], N. Nègre[a], M. Goiran[a], C. Guerret-Piécourt[b]

[a] *Laboratoire de Physique de la Matière Condensée de Toulouse, INSA. SNCMP, Universite Paul sabatier, Complexe Scientifique de Rangueil, 31077 Toulouse Cedex 4, France*

[b] *LAAS-CNRS, 7 av. du Colonel Roche, 31077 Toulouse Cedex, France*

Received 28 July 1997; received in revised form 7 November 1997

Abstract

The results of the preparation, characterization and magnetic properties of a CoO/Co interface are discussed. This interface was realized by ultraviolet irradiation of a 4 nm Co layer deposited with a gold buffer layer on a GaAs(1 1 1) substrate. The Co oxide analyzed by XPS and AFM revealed a continuous 1.7 nm thick layer with a rms roughness of 0.6 nm and mostly CoO at the interface. Longitudinal magneto-optical Kerr loops evidence a strong initial in-plane anisotropy which disappears on oxidation. Values of the unidirectional exchange coupling at the Co/CoO interface were obtained: 0.1 erg/cm^2 from SQUID measurement at 5 K after field cooling and 0.6 erg/cm^2 with magneto-optical Kerr effect in polar configuration from modelization of the $M(H)$ curve. This discrepancy is discussed in terms of the difference of sensing the interfacial coupling in the two cases due to atomic steps. © 1998 Elsevier Science B.V. All rights reserved.

PACS: 75-60; 75-70; 81-15G

Keywords: Exchange coupling; Anisotropy – uniaxial; Anisotropy – unidirectional; Thin films

1. Introduction

We present a study of the preparation and characterization of the antiferro/ferromagnetic CoO/Co interface. The knowledge of the insulating-magnetic nature of an ultra-thin CoO layer as well as the magnetic coupling (exchange anisotropy) may be very useful to realize spin-dependent tunneling devices [1,2] and spin-valve structures with pinned layers [3,4]. Their use in magnetoresistive random access memories (MRAM) is also called for question [5]. The best interface arises from (1 1 1) orientation with alternating ferromagnetic sheets of CoO [6]. However, actual insulating layers suffer from lack of homogeneity, roughness and crystallinity. To get a better quality of the oxide layer, we propose an ultra-violet (UV) oxidation method (UVOX) that seems to be in our case quite satisfactory. Co was deposited on a gold buffer layer on a GaAs(1 1 1) substrate. The CoO/Co interface was realized by air UVOX. The chemical analysis confirms the CoO nature of the interfacial oxide. An obvious proof of the antiferromagnetic nature of the oxide is given by the shift of the magnetic loops which appears below the Néel temperature of the

* Corresponding author. Tel.: + 33 5 61 55 61 85; e-mail: mamy@insa-tlse.fr.

0304-8853/98/$19.00 © 1998 Elsevier Science B.V. All rights reserved.
PII S0304-8853(97)01105-0

oxide layer and gives by the way an evaluation of the interfacial exchange anisotropy. Finally, this exchange energy is also extracted from the magnetization measurement of the Co/CoO bilayer along the normal direction of the film.

2. Experiment

The GaAs surface was obtained by homoepitaxy from a nominal (1 1 1)GaAs wafer in a MBE apparatus [7] and furnished covered with a passivation As cap in the metal deposition chamber where it was reacted by heating so as to obtain a (2×2) surface reconstruction. A 20 nm gold and 4 nm Co layers were sequentially deposited at room temperature by thermal evaporation [8]. We chose to oxidize the Co layer by UVOX (ozone generation) which has already proven efficient in semiconductor technology [9]. The chemical analysis was performed using electron spectroscopy for chemical analysis (ESCA) with a commercial apparatus from vacuum generators (VG) using non-monochromatized Mg Kα radiation. The atomic force microscopy (AFM) images were obtained from a Nanoscope III® apparatus from Digital Instruments Inc. The magnetic hysteresis loops were measured at room temperature with a magneto-optical Kerr effect magnetometer and at low temperature (5 K), with a SQUID magnetometer. Another magneto-optical Kerr effect apparatus [10] with a pulsed high magnetic field was used in polar configuration down to 5 K.

3. Uniaxial in-plane anisotropy

We report the study of the in-plane magnetic switching behavior of the Co (4 nm) film performed by longitudinal magneto-optical Kerr effect. The magnetization measurements were realized ex situ and at room temperature just after the preparation. Our follow-up of the time-dependent oxidation of the Co layer in air ensures the negligible alteration of the uncovered Co layer two days after the exposure in air. The lack of oxidation at the beginning of the exposure in air reveals the high crystallographic quality of the uncovered magnetic layer.

Fig. 1a–Fig. 1c show three typical M-H curves illustrating the magnetic anisotropy in the plane of the layer. The angle θ_H defines the direction of the magnetic field with respect to the [1 1 0] crystallographic directional axis of the GaAs(1 1 1). The MOKE intensity is normalized to the Kerr rotation obtained in the saturated state. We first observe unambiguously a strong unexpected in-plane uniaxial anisotropy with the easy-axis along a well-defined crystallographic direction [1 1 0] of the GaAs(1 1 1) substrate. The easy-axis loop (Fig. 1a) presents an approximate square-loop revealing a small angular distribution of the easy direction of around $\pm 15^\circ$. However, the lack of hysteresis for an applied magnetic field perpendicular to the easy-axis suggests the high film quality and the uniaxial nature of the in-plane anisotropy, which dominates over higher-order anisotropies.

The in-plane uniaxial anisotropy constant K_u is easily estimated using a coherent rotation model [11–13] in a restricted range of θ_H and H values. We reasonably assume that the magnetization behavior is dominated by a reversible coherent rotation for a decreasing magnetic field from the saturation field H_s to 0 with the angle θ_H between the field and the easy-axis inferior to 40°. For the Co (4 nm) layer discussed in this paper, we find that it is sufficient to include only the uniaxial anisotropy term K_u and the Zeeman energy to express the total magnetic energy

$$E_t = K_u \sin^2(\theta) - HM_s \cos(\theta - \theta_H), \quad (1)$$

where θ and θ_H are the angles defining, respectively, the orientation of the magnetization and the applied field with the easy axis. The shape anisotropy energy is large enough to favor in-plane magnetization, we therefore assume the reversal process confined to the film plane. Besides, we neglect any magneto-crystalline contribution in the (0 0 0 1) HCP plane of the cobalt compared to the strength of the observed uniaxial anisotropy.

The magnetization curves are obtained by minimizing Eq. (1) with respect to θ and for a fixed orientation of the applied field. Fig. 1d shows two examples of the calculated magnetization as solid lines in good agreement with the experimental measurements corresponding to $\theta_H = 24.5$ and 37°. The only one parameter K_u is adjusted in order to

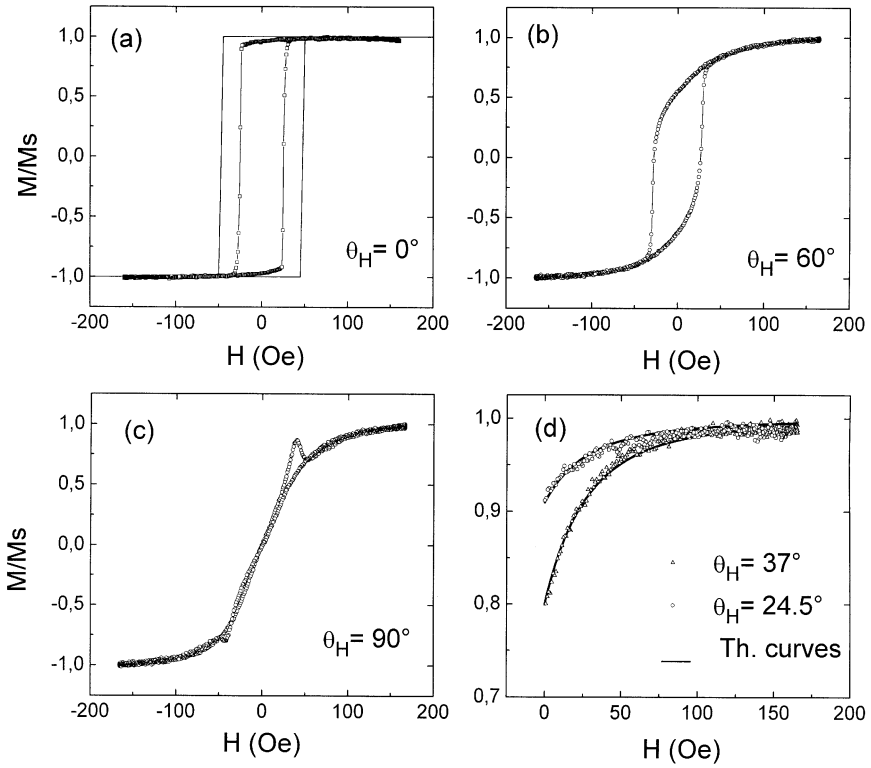

Fig. 1. (a)–(d). Longitudinal magneto-optical Kerr loops for different values of the angle θ_H between the direction of the magnetic field in the plane of the (1 1 1) surface and the [1 1 0] crystallographic direction of the GaAs substrate. The fitting with a coherent rotation model is shown in solid lines in (a) and (d).

obtain the best fit. Whatever the value of θ_H, we deduce the same value of $K_u = 3.6 \times 10^4$ erg/cm^3.

It is noticeable that such a well-defined anisotropy is absolutely neither owing to a magneto-crystalline direction, contrary to experimental results observed in Co(BCC)/GaAs(0 0 1) [14] or Fe/Ag(100) [15] and not induced by a step bunching phenomena on a vicinal surface. The uniaxial anisotropy constant deduced from our measurements is at least 40% greater than the in-plane uniaxial anisotropy estimated in other Co thin layers deposited on nominal surfaces [14].

Before deposition of Au(1 1 1) at room temperature, the GaAs(1 1 1) surface is analyzed by AFM. Some regular atomic steps at the surface are observed along the [1 1 0] crystallographic direction of the substrate (Fig. 2). By scanning the Au(20 nm) deposited on GaAs(111), the AFM image reveals the persistence of a stepped topography along the same axis. We therefore attribute the strong uniaxial in-plane anisotropy of the Co layer to a shape memory of the substrate, which disturbs the Au/Co interface on an atomic scale. Previous studies dealing with the origin of such an unexpected uniaxial in-plane anisotropy provide insight into the contribution of atomic steps of the substrate to the magnetic anisotropy [15–17]. A lateral pseudo-periodic variation of the interfacial topography may induce, among other things, a shape anisotropy of the Co islands within the film or an oriented residual strain in the magnetic layer. A microstructural study by transmission electron microscopy is in progress to clarify the effects of the atomic steps on the growth of the Co layer.

Let us remark the large discrepancy between the theoretical magnetization curve (Fig. 1a, solid line)

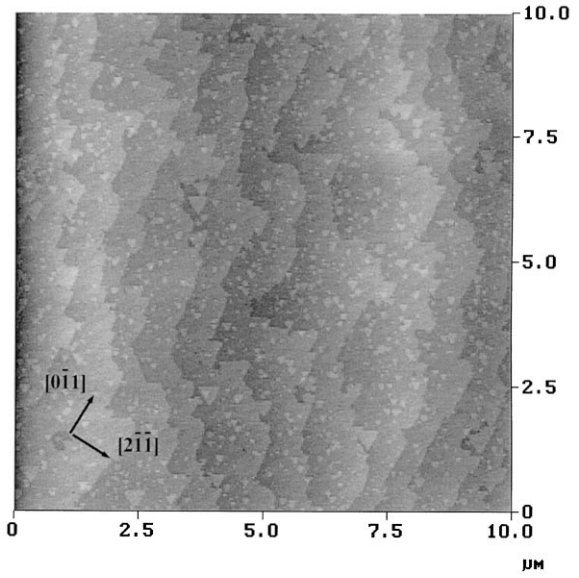

Fig. 2. AFM topography (10 μm × 10 μm) of the GaAs(1 1 1) surface showing the atomic steps along the [0 −1 1] direction.

and the experimental loop when the field is applied along the easy axis ($\theta_H \approx 0^\circ$). The switching behavior is most likely to deviate from the coherent rotation model. A dynamical study of the magnetization and relaxation experiments along the [1 1 0] substrate direction presented evidence that the magnetization reversal is largely dominated by the domain-wall motion process [18].

4. Characteristics of the oxidization process

We followed the evolution of the oxidization process of a sample left in air over weeks as compared to another sample submitted to an UV irradiation during 15 min. In the air oxidation case, the Kerr intensity and the uniaxial anisotropy regularly decrease while the hysteresis loops broaden (Fig. 3a and inset), in the UV oxidation case the uniaxial anisotropy completely disappears and the hysteresis loops broaden even more (Fig. 3b). The AFM image of the UV oxidized surface (Fig. 4) shows a continuous oxide layer with a root mean square (rms) roughness of 0.6 nm while oxidation in air gives oxide patches. So UV oxidation turns out as a more rapid and suitable method.

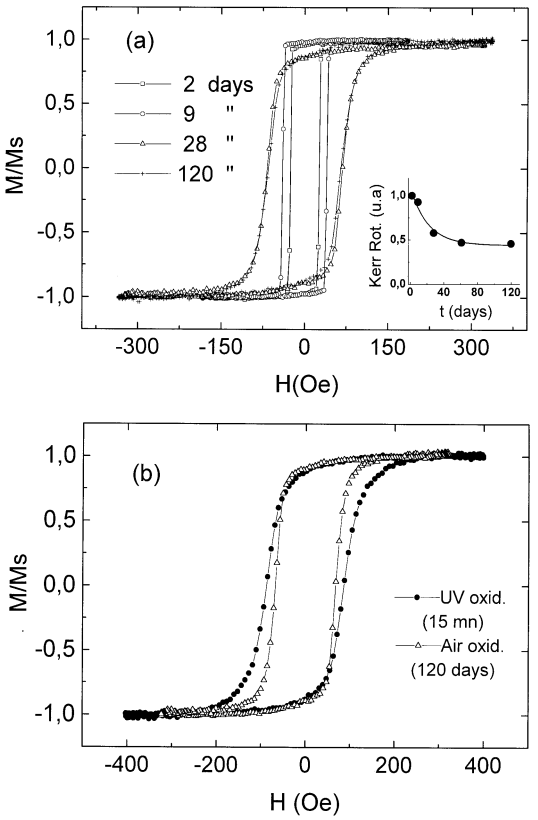

Fig. 3. (a) Evolution of the longitudinal magneto-optical Kerr loops performed at room temperature for the 4 nm Co layer as a function of the number of days exposed to air. The attenuation of the Kerr intensity is shown in the inset. (b) Comparison of the effect of a 15 min UV exposure with respect to 120 d in air on longitudinal magneto-optical Kerr loops.

The slow air oxidation process can be brought together with other studies of kinetics of ultra-thin Co layers [19] which give a thickness-dependent process: very rapid oxidation (however limited to 2.5 nm of oxide) for thickness >5 nm and very long time constants for lower thickness. As the Kerr measurements plotted in Fig. 3 are performed at room temperature, the Kerr intensity is mainly proportional to the Co thickness. The solid line in inset of Fig. 3a represents an exponential fit of the air oxidation process as a function of time. The decay rate of oxidation is estimated to 22 d which is in good agreement with the previous works [19].

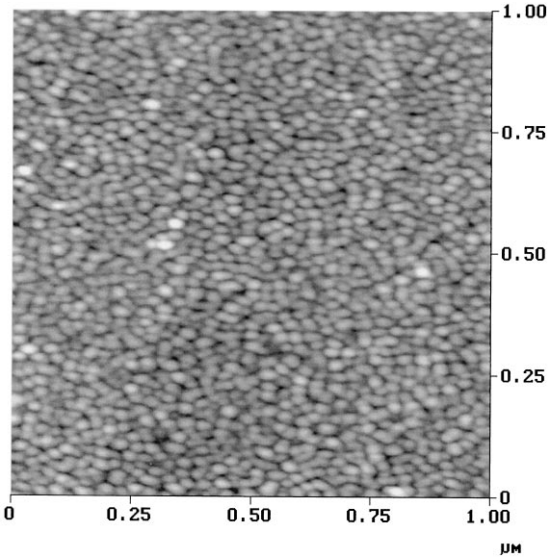

Fig. 4. AFM topography (1 μm × 1 μm) of the CoO surface after UV irradiation (15 min), the measured RMS roughness is 0.6 nm.

5. Analysis of the oxide layer

ESCA is a powerful technique to determine the oxidation number and the thickness of the oxide from the analysis of the core state shifts (namely Co_{2p} and O_{1s} here). Moreover, the different spin configuration of Co^{II} (para and high-spin configuration) and Co^{III} (dia and low-spin configuration) ions permits the identification of CoO which presents a strong satellite shake-up structure on the Co 2p states which is considerably weaker in the Co_3O_4 case [20,21]. We present in Fig. 5 the $Co_{2p3/2}$ and $Co_{2p1/2}$ region for the UV oxidized sample which shows the satellite structure (786 eV) of the $Co_{2p3/2}$ peak (780.5 eV) and which identify unambiguously CoO. Each Co2p peak has unresolved oxidized and non-oxidized component 2 eV wide which gives after line-shape analysis following classical methods [22] a 1.7 m oxide thickness. Useful information can also be extracted from the O_{1s} peak which exhibits two components at 529.5 (I) and 531 eV (II). Although the interpretation of these components in the Co oxide case is disputed [23] it seems that the less intense component I, is due to CoO and the other to non-stoichiometric

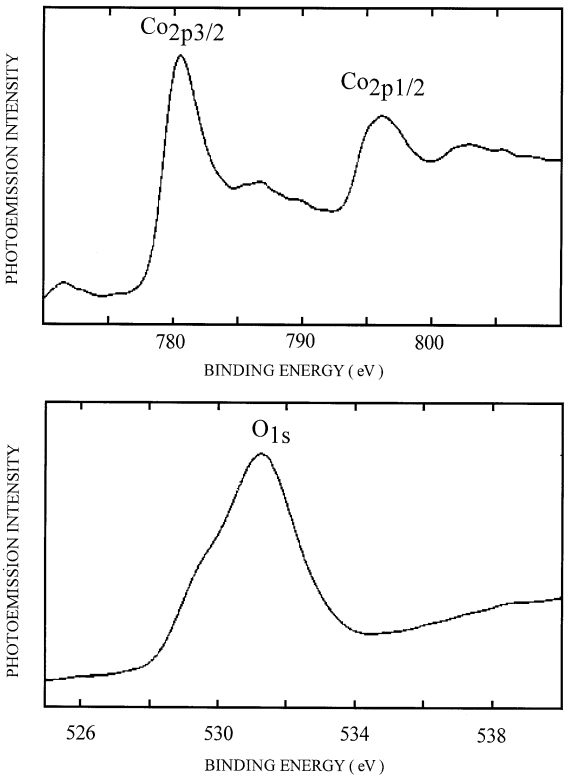

Fig. 5. XPS spectra of (a) the Co_{2p} and (b) the O_{1s} core levels.

surface region [20]. In fact the angular variation of the O_{1s} peak shows that the intensity of the peak I decreases towards grazing angle and consequently arises from underneath the oxide layer, i.e. near the interface. Finally, starting from a 4 nm Co thickness, the UV oxidization turns 1.7 nm into oxide and the interfacial part is pure CoO.

6. Unidirectional exchange anisotropy

The antiferromagnetic behavior of the oxide overlayer is borne out by measuring hysteresis loops in the temperature range from 5 to 300 K, by SQUID magnetometer.

Fig. 6a shows two hysteresis loops for the oxidized film performed at 5 K, to which the sample was cooled from 300 K in a demagnetized state and below which a magnetic field of 50 kOe was applied parallel to the film plane.

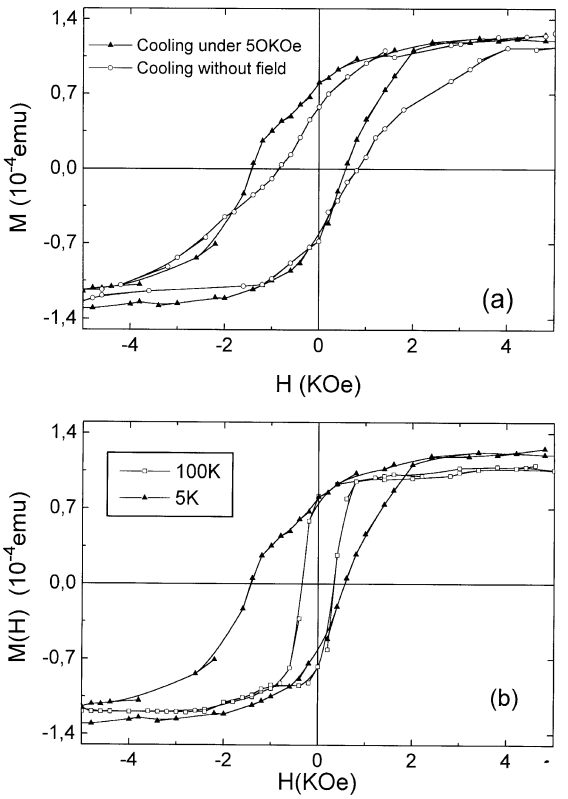

Fig. 6. (a) Comparison of SQUID hysteresis loops for CoO/Co cooled without and under an applied field. The field-cooled loop is shifted by an offset field of -420 Oe. (b) Field-cooled SQUID loop taken above (100 K) and below (5 K) the Néel temperature of CoO.

Under the last condition, an unidirectional exchange anisotropy is manifested by a negative field offset H_{off} of -420 Oe, defined as

$$H_{off} = (|H_c^1| - |H_c^2|)/2,$$

where H_c^1 and H_c^2 are the coercive fields corresponding, respectively, to the left and right sides of the loop. No shift is observed on the hysteresis loop when the sample is cooled in the absence of an applied field. It is well known that the shifted magnetization is induced by the antiferromagnetic/ferromagnetic exchange coupling at the CoO/Co interface [24]. The high magnetic field of 50 kOe is applied during the cooling to obtain a single antiferromagnetic domain in the CoO. Fig. 6b compares the hysteresis loops for the oxidized film cooled from 300 K in a positive magnetic field of 50 kOe and performed at two distinct temperatures 5 and 100 K. The centered hysteresis loop obtained at 100 K reveals that the Néel temperature of the CoO/Co layer is below this temperature. It is in agreement with our estimated CoO thickness by XPS and the known Néel temperature dependence on the CoO thickness [25].

The exchange energy per unit area of the interface J_i can be explicitly calculated as the field offset H_{off} has been shown to follow the relation [19]

$$H_{off} = \frac{J_i}{M_s t_{Co}}. \quad (2)$$

The thickness of the non-oxidized Co underlayer t_{Co} is roughly estimated considering the absolute value of the saturation magnetization measured by SQUID. We deduce approximately a 2 nm Co layer thickness. This value is consistent with the thickness of the oxide layer estimated by XPS. Inserting $M_s \sim 1.833$ T, the Co bulk value of the saturated magnetization in Eq. (2), we obtain, $J_i = 0.12$ erg/cm^2. This exchange constant is in the same order of magnitude of those defined in previous works in CoO/Co bilayers [6,19,26,27]. However, one usually notices a large scatter of the experimental exchange coupling values as the strength of the exchange AF/F drastically depends on the structural quality of the CoO/Co interface.

Therefore, we propose another experiment to analyze the effect of the interface roughness on the exchange coupling Co/CoO per unit of area. In a polar configuration, we measure at 5 K the perpendicular magnetization of the Co layer in an high pulsed magnetic field perpendicular to the layer. The results given in Fig. 7 show the effect of the oxide layer on the magnetization behavior of the Co along the [0 0 0 1] axis. As the field needed to rotate the CoO magnetic moments in the bulk is around 380 T, we consider that in our range of applied field, the CoO magnetic moments keep blocked in the plane of the layer. Thus, assuming a coherent rotation process along the hard axis, the total energy can be simply expressed as follows:

$$E_t = K_{eff} \sin^2(\theta) - M_s H \cos(\theta) - J_i/t_{Co} \sin(\theta), \quad (3)$$

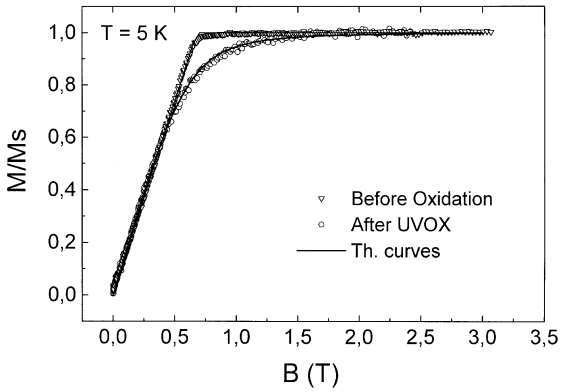

Fig. 7. Magnetization curves performed at 5 K in polar configuration along the hard direction (normal to surface of the sample) before and after oxidation. The fit with a coherent rotation model is shown in solid lines.

where θ defines the angle between the normal axis and the magnetization.

The first term is the effective perpendicular anisotropy of the Co layer, the second corresponds to the Zeeman energy and the last term accounts for the exchange coupling energy at the CoO/Co interface. Before oxidation, the experimental magnetization curve is easily fitted without considering the exchange coupling. We find K_{eff} equal to -5×10^6 erg/cm^3. After UV oxidation, the two parameters deduced from the best fit, by minimizing Eq. (3) with respect to θ, are $K_{\text{eff}} = -2.64\times10^6$ erg/cm^3 and $J_i = 0.67$ erg/cm^2. The effective perpendicular anisotropy affects the slope of the Co magnetization in low magnetic field, whereas, the strength of the exchange coupling causes the difficult saturation of the cobalt. It is surprising to remark that the exchange coupling deduced from the polar configuration is increased by a factor 6, compared to the exchange energy measured in a longitudinal configuration. In fact, the experiment in polar configuration allows to estimate the real intensity of the coupling, independently of the magnetic multidomain structure of the CoO induced by the interface steps. A simple calculus shows that, despite the cooling under 50 kOe, 40% of the exchange surface between CoO/Co has got adjacent CoO moments opposite to the applied positive magnetic field, due to the interfacial atomic steps. Such a magnetic arrangement drastically decreases the effect of the exchange coupling measured in the longitudinal configuration of the applied magnetic field.

7. Conclusions

The ultra-violet oxidation method that we proposed to realize CoO/Co interface proved to be better than oxidation in air as concerns the homogeneity and roughness of the oxide layer. The difference in the values of the unidirectional exchange coupling obtained for the in-plane and perpendicular field directions in the hysteresis loops can be accounted for by the fact that for in-plane field the unidirectional exchange field is locally suppressed by alternation of the magnetization at monoatomic steps. This can be an indirect method to check the interfacial roughness or to test any method intended to improve the interfacial roughness.

Acknowledgements

We acknowledge the services of the Ecole Nationale Supérieure de Chimie and the Laboratoire de Chimie de Coordination de Toulouse for ESCA and SQUID measurements.

References

[1] J.S. Moodera, L.R. Kinder, J. Appl. Phys. 79 (1996) 4724.
[2] P. Leclair, J.S. Moodera, R. Meservey, J. Appl. Phys. 76 (1994) 6546.
[3] M.J. Carey, A.E. Berkowitz, Appl. Phys. Lett. 60 (1992) 3060.
[4] T. Lin, C. Tsang, R.E. Fontana, J.K. Howard, IEEE Trans. Magn. 31 (1995) 2585.
[5] E.Y. Chen, S. Tehrani, T. Zhu, M. Durlam, H. Goronkin, J. Appl. Phys. 81 (1971) 3992.
[6] J. Bransky, I. Bransky, A.A. Hirsch, J. Appl. Phys. 41 (1970) 183.
[7] B.J. Garcia, C. Fontaine, A. Muñoz-Yagüe, Appl. Phys. Lett. 66 (1995) 610.
[8] R. Mamy, Surf. Sci. 322 (1995) 337.
[9] E. Bedel, A. Muñoz-Yagüe, C. Fontaine, C. Vieu, Mater. Sci. Eng. B 21 (1993) 157.
[10] M. Goiran, N. Nègre, S. Jaren, C. Meyer, R. Barbaste, A.R. Fert, J.C. Ousset, S. Askénazy, Physica B, to be published.

[11] E.C. Stoner, E.P. Wohlfarth, Philos. Trans. A 240 (1948) 599.
[12] B. Dieny, J.P. Gavignan, J.P. Rebouillat, J. Phys.: Condens. Matter 2 (1990) 159.
[13] V. Grolier, Ph.D. Thesis, Orsay, 1994.
[14] J.A.C. Bland, M.J. Baird, H.T. Leung, A.J.R. Ives, K.D. Mackay, H.P. Hughes, J. Magn. Magn. Mater. 113 (1992) 178.
[15] M. Gester, C. Daboo, R.J. Hicken, S.J. Gray, A. Ercole, J.A.C. Bland, J. Appl. Phys. 80 (1996) 347.
[16] M. Albrecht, T. Furubayashi, M. Przybylski, J. Korecki, U. Gradmann, J. Magn. Magn. Mater. 113 (1992) 207.
[17] J. Fassbender, C. Mathieu, B. Hillebrands, G. Güntherodt, R. Jungblut, M.T. Johnson, J. Magn. Magn. Mater. 148 (1995) 156.
[18] B. Raquet, R. Mamy, J.C. Ousset, unpublished.
[19] L. Smardz, U. Köbler, W. Zinn, J. Appl. Phys. 71 (1992) 5199.
[20] T.J. Chuang, C.R. Brundle, D.W. Rice, Surf. Sci. 59 (1976) 413.
[21] C.R. Brundle, T.J. Chuang, D.W. Rice, Surf. Sci. 60 (1976) 286.
[22] T.A. Carlson, G.E. McGuire, J. Electron. Spectrosc. Relat. Phenom. 7 (1975) 175.
[23] K. Wandelt, Surf. Sci. Rep. 2 (1982) 1.
[24] W.H. Meiklejohn, C.P. Bean, Phys. Rev. 102 (1956) 1413.
[25] T. Ambrose, C.L. Chien, Phys. Rev. Lett. 76 (1996) 1743.
[26] H. Danan, H. Gengnabel, J. Steinert, A. Linzen, J. de Phys. 32 (1971) C1.
[27] M. Takahashi, A. Yanai, S. Tagushi, T. Suzuki, Jpn. J. Appl. Phys. 19 (1980) 1093.